A Novel Feasible Parameter Region-based Approach for Transmission Line Parameter Error Identification and Correction

Meng-Lu Zhu
School of Electrical and Information Engineering
Tianjin University
Tianjin, China

Hsiao-Dong Chiang, *Fellow*, *IEEE*
School of Electrical and Computer Engineering
Cornell University
Ithaca, NY, USA

Dong Liang, *Member*, *IEEE*
School of Electrical Engineering
Hebei University of Technology
Tianjin, China

***Abstract*—The accuracy of transmission line parameters (e.g., line impedances) is critical for power system analysis, computation and optimization. This paper derives a complete characterization for the feasible parameter region (FPR) of the set of line parameters and proposes an FPR-based method for parameter error identification and correction problem. Theoretically speaking, the FPR provides an effective analytical basis for identifying transmission line parameter errors. Numerically speaking, a three-stage framework comprising screening stage, ranking stage and detailed analysis stage is established for parameter error identification and correction (PEIC). Several numerical tests reveal that the proposed three-stage numerical method is effective to identify both the issues of non-adjacent and adjacent parameter errors and to obtain correct parameter values. The verification of these corrections was performed based on the accuracy improvement of state estimation after the correction over a range of state estimation results (say, over 200 snapshots).**

***Index Terms*—Feasible parameter region, parameter error identification and correction, parameter estimation.**

I. INTRODUCTION

As the basic foundation for all advanced energy management systems (EMS) applications [1], state estimation (SE) is influenced by the quality of measurement data and the accuracy of power system model parameters. However, it is known that discrepancies can exist between line parameter values recorded in the databases and the actual parameters values, originating from inaccurate equipment data, parameter drift due to long-term aging or environmental changes, and outdated records [2]. Hence, the identification and correction of these erroneous parameters is therefore necessary, serving as a critical prerequisite for reliable state estimation.

Prevailing approaches for parameter estimation (PE) generally fall into two categories: 1) Residual sensitivity analysis-based methods [3]-[5], which formulate the estimation problem by analyzing the sensitivity of SE residuals to parameter changes and directly correct the parameter errors; and 2) State vector augmentation-based methods [6]-[8], which augment the state vector with the suspicious parameters and perform a joint estimation alongside the system operating states. Although the alternative approach based on the normalized Lagrange multiplier (NLM) [9] has shown promise in identifying both single and multiple noninteracting parameter errors [10], its performance in scenarios with interacting parameter errors requires further investigation. The advent of phasor measurement units (PMUs) has spurred the development of parameter estimation methods that leverage their high-precision, time-synchronized data [11].

This paper proposes a novel analytical and numerical framework for line parameter error identification and correction (PEIC). The main contributions are summarized as follows:

(1) A theoretical characterization for feasible parameter region (FPR) of the PEIC problem is derived.

(2) A robust FPR-based method is proposed for erroneous parameter identification and demonstrated its ability to significantly reduce the dependence on the precision of a priori suspicious parameter set and effectively mitigates misidentification risks.

(3) A novel three-stage framework comprising screening, ranking and detailed analysis stage is developed for the identification and correction of parameter errors, enabling accurate identification and correction of multiple non-adjacent and adjacent parameter errors.

II. FEASIBLE PARAMETER REGION OF BOUNDED PARAMETER ESTIMATION

The nonlinear measurement model relating to the measurement vector $\boldsymbol{z}$ and state vector $\boldsymbol{x}$ is given by:

$$\boldsymbol{z} = \boldsymbol{h}(\boldsymbol{x}) + \boldsymbol{v} \tag{1}$$

where $\boldsymbol{v}$ is the measurement error vector, and $\boldsymbol{h}$ is the measurement function, derived from the AC power flow equations, representing a nonlinear mapping from $\boldsymbol{x}$ to $\boldsymbol{z}$ [2].

Considering the transmission line parameters, which include line resistance r, reactance x and shunt susceptance b, the measurement equation in PE based on the SE results can be formulated in a similar form as:

$$\boldsymbol{z} = \boldsymbol{g}(\boldsymbol{p}) + \boldsymbol{v} \tag{2}$$

where $\boldsymbol{p}$ is the parameter vector, and $\boldsymbol{g}$ is the measurement function, which represents a nonlinear mapping from the parameter vector to the measurement vector.

The weighted least squares (WLS) estimator is used in PE.

$$\min J(\boldsymbol{x}) = \left[\boldsymbol{z} - \boldsymbol{g}(\boldsymbol{p})\right]^{\mathrm{T}} \boldsymbol{R}^{-1} \left[\boldsymbol{z} - \boldsymbol{g}(\boldsymbol{p})\right] \tag{3}$$

where $\boldsymbol{R}^{-1}$ is the weighting matrix. The state variables are obtained from SE.

A feasible parameter solution $\boldsymbol{p}$ is subject to the set of residual constraints:

$$\left|z_i - g_i(\boldsymbol{p})\right| \le L_i \quad i \in \{1,\ldots,m\}, \boldsymbol{p} \in \Re^{N_p} \tag{4}$$

where L_i is the bound of each residual constraint, which defines the permissible deviation for the measurement. The set of residual constraints collectively characterize the range within which the true values of the line parameters are expected to lie. Each L_i is often available from the manufacturer.

979-8-3315-8138-1

The difference between the measurements z and the estimated results represented by $g(p)$ is constrained in formulation (4), which is referred to as the bounded parameter estimation (BPE) problem in this paper.

For simplicity, rewrite inequalities (4) in a compact form as:

$$C_I\left(p, g(p)\right) \le \mathbf{0} \quad p \in \Re^{N_p} \tag{5}$$

The set of inequality residual constraint functions of the BPE problem can be transformed into equality constraints by introducing slack variables s:

$$H(y) = \left[C_I(p) + s^2\right] = \mathbf{0} \tag{6}$$

where $H: \Re^{N_p} \to \Re^m$, $y = (p, s) \in \Re^{N_p+m}$, $s^2 = (s_1^2, \ldots, s_m^2)^{\mathrm{T}}$.

To characterize the feasible solution of the BPE problem, the definition of the feasible parameter region building upon the above formulation of the BPE problem is presented below.

Definition 1: (The feasible parameter region)

The feasible parameter region (FPR) is a set of parameter variables for which all the residual constraints of the BPE problem are satisfied, i.e.,

$$FPR = \left\{ p \in \Re^{N_p} : H(y) = H(p, s) = \mathbf{0} \right\} \tag{7}$$

To characterize the FPR, we consider a nonlinear and non-hyperbolic dynamic system built according to (4):

$$\dot{y} = Q_H(y) = -DH(y)^{\mathrm{T}} H(y) \tag{8}$$

where DH is the Jacobian matrix of $H(y)$. System (8) is termed the quotient gradient system (QGS) associated with (6).

Next, a brief overview of some concepts related to the QGS systems is provided. A detailed description of these concepts can be found in [12].

Definition 2: (Equilibrium manifold)

For system (8), its equilibrium manifold (EM) Σ is the path-connected component of the set $Q_H^{-1}(\mathbf{0})$. Specifically, every point of an EM satisfies $Q_H(y) = \mathbf{0}$.

Definition 3: (Regular stable equilibrium manifold)

It is a stable equilibrium manifold (SEM) Σ_s if, for each $y \in \Sigma_s$, the real part of the eigenvalues of $DH(y)$ whose corresponding eigenvectors in the normal space are all negative. If a SEM Σ_s satisfies $DH(\Sigma)^{\mathrm{T}} H(\Sigma) = \mathbf{0}$ and $H(\Sigma) \neq \mathbf{0}$, it is a regular stable equilibrium manifold (RSEM) Σ_{rs}; otherwise, if $DH(\Sigma)^{\mathrm{T}} H(\Sigma) = \mathbf{0}$ and $H(\Sigma) \neq \mathbf{0}$, it is a degenerate stable equilibrium manifold (DSEM) Σ_{ds}.

Theorem 1: (Feasible parameter region and RSEM)

A FPR satisfies the residual constraint set (4) of the BPE problem if and only if it is an RSEM of QGS (8), i.e.,

$$FPR = \Sigma_{rs} \tag{9}$$

Due to space limitations, the proof is omitted; a similar proof regarding the correspondence between the feasible region and the RSEM can be found in [12].

As shown in *Theorem 1*, the feasible solution to the constraint set (4) can be found by tracking the RSEM of QGS (8). The presence of the energy function determines the asymptotic characteristics of the trajectories of QGS (8), guaranteeing the global convergence of the proposed QGS-based method.

To illustrate the concept of the FPR and demonstrate the proposed QGS-based method, the FPR of the 2-bus system is characterized.

The QGS of the test 2-bus system is formulated as:

$$\dot{y} = Q_H(y) = -DH_{2\text{-}bus}(y)^{\mathrm{T}} H_{2\text{-}bus}(y) \tag{10}$$

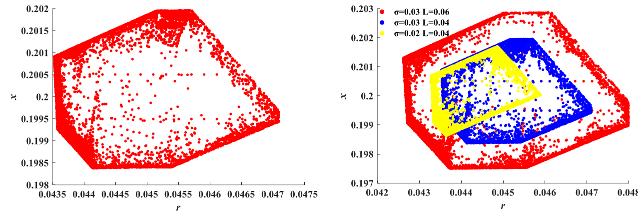

(a) (b)

Figure 1. The FPR of the 2-bus system. Active set is employed to characterize the boundary of the FPR. (a) The FPR of the 2-bus system is equivalent to the RSEM of the QGS (10). (b) The FPR corresponds to different constraint boundaries and standard deviations.

The RSEM of the QGS coincides with the FPR, as illustrated in Fig. 1. When the network topology and parameters remain unchanged, adjustments to the residual constraint boundaries and the standard deviation σ lead to alterations in the FPR. The FPR is also influenced by the specific set of measurements.

III. Parameter Error Correction Method

A novel PEIC method, comprising three stages: screening, ranking, and detailed analysis is proposed in this section. The numerical techniques for each stage of the proposed three-stage methodology are presented below.

A. Stage 1 Screening

To fast screen out suspicious parameters, a linear method based on the parameter-residual sensitivity is employed.

The parameter error vector p_e to be estimated is defined as the deviation of the recorded parameter value vector p_r from the true parameter value vector p_t:

$$p_e = p_r - p_t \tag{11}$$

If parameter errors exist, the measurement equation for SE (1) is rewritten as follows:

$$z = h(x, p_e) + v \tag{12}$$

The linearized expression of (12) around an operating point is formulated as [10]:

$$\Delta z' = H\Delta x' + H_p p_e + v = K\Delta z + SH_p p_e \tag{13}$$

where $\Delta z'$ is the actual increment of the measurement vector; $H = \partial h/\partial x$ is the Jacobian matrix of the measurement function with respect to the state vector; $H_p = \partial h/\partial p$ is its Jacobian matrix with respect to the parameter errors.

Meanwhile, the true linearized measurement model without parameter errors, can be written as:

$$\Delta z = H\Delta x + v \tag{14}$$

Combining (13) and (14), the residual r can be expressed as:

$$r = \Delta z - \Delta z' = -SH_p p_e + Sv = Bp_e + Sv = Bp_e + \tau \tag{15}$$

where $\tau \sim N(0, SRS^{\mathrm{T}})$ represents the measurement noise, $B = -SH_p$ is the parameter-residual sensitivity matrix, which quantifies the sensitivity of r to p_e.

The objective is to determine a set of parameter error estimates p_e, such that the theoretically induced residual minimizes the discrepancy with the observed residual vector, which defines a least-squares optimization problem:

$$\min_{p_e} J = (r - Bp_e)^{\mathrm{T}} \Lambda_\tau^{-1} (r - Bp_e) \tag{16}$$

979-8-3315-8138-1

where $\Lambda_\tau = \boldsymbol{SRS}^{\mathrm{T}} + \delta\boldsymbol{I}$, δ is introduced to ensure the invertibility of the matrix. Its value is typically chosen to be 2~3 orders of magnitude smaller than the standard error deviations and is set to 10^{-5} for the initial screening stage.

Deriving the optimal solution based on the first-order optimality condition yields:

$$\hat{\boldsymbol{p}}_{\mathrm{e}} = (\boldsymbol{B}^{\mathrm{T}}\Lambda_\tau^{-1}\boldsymbol{B})^{-1}\boldsymbol{B}^{\mathrm{T}}\Lambda_\tau^{-1}\boldsymbol{r} \tag{17}$$

Calculate the variance:

$$\mathrm{Var}(\hat{\boldsymbol{p}}_{\mathrm{e}}) = \mathrm{Var}\left(\frac{\boldsymbol{B}^{\mathrm{T}}\Lambda_\tau^{-1}\boldsymbol{r}}{\boldsymbol{B}^{\mathrm{T}}\Lambda_\tau^{-1}\boldsymbol{B}}\right) = \frac{\mathrm{Var}(\boldsymbol{B}^{\mathrm{T}}\Lambda_\tau^{-1}\boldsymbol{r})}{(\boldsymbol{B}^{\mathrm{T}}\Lambda_\tau^{-1}\boldsymbol{B})^2} = \frac{1}{\boldsymbol{B}^{\mathrm{T}}\Lambda_\tau^{-1}\boldsymbol{B}} \tag{18}$$

To rapidly screen out suspicious parameters in the screening stage, a statistical hypothesis testing framework is developed.

$$H_0 : p_{\mathrm{e},j} = 0 \quad H_1 : p_{\mathrm{e},j} \neq 0 \tag{19}$$

A test statistic T is formulated as:

$$T_j = \frac{\hat{p}_{\mathrm{e},j}}{\sqrt{\mathrm{Var}(\hat{p}_{\mathrm{e},j})}} = \frac{\hat{p}_{\mathrm{e},j}}{\sqrt{[(\boldsymbol{B}^{\mathrm{T}}\Lambda_\tau^{-1}\boldsymbol{B})^{-1}]_{jj}}} \sim N(0,1) \tag{20}$$

A large absolute value of T_j indicates that the observed residual pattern is highly consistent with what would be expected from an error in parameter p_j.

The probability of obtaining a T-value exceeds the critical value, given that the null hypothesis H_0 is true, is:

$$\varphi_j = P(|T_j| > |t_{\mathrm{obs}}| \,|\, H_0) = 2(1 - \Phi(T_j)) \tag{21}$$

When φ_j is less than the significance level α, it provides strong evidence to reject the null hypothesis H_0, indicating the presence of parameter errors.

Given that parameter errors persist while bad data measurements occur sporadically, leveraging multiple-snapshot data can effectively highlight consistently anomalous parameters while mitigating random noise.

In the presence of N snapshots, residual becomes:

$$\begin{bmatrix} \boldsymbol{r}_1 \\ \boldsymbol{r}_2 \\ \vdots \\ \boldsymbol{r}_N \end{bmatrix} = \begin{bmatrix} \boldsymbol{B}_1 \\ \boldsymbol{B}_2 \\ \vdots \\ \boldsymbol{B}_N \end{bmatrix} \boldsymbol{p}_{\mathrm{e}} + \begin{bmatrix} \boldsymbol{\tau}_1 \\ \boldsymbol{\tau}_2 \\ \vdots \\ \boldsymbol{\tau}_N \end{bmatrix} \tag{22}$$

Following the multiple-snapshot analysis, parameters whose φ exceed a significance level α constitute the suspicious parameter set *SP*.

B. Stage 2 Ranking

To accurately identify erroneous parameters, the ranking of suspicious parameters is performed based on the FPR. When the true value of a parameter differs from the value recorded in the databases, a discernible offset emerges between the FPR and the recorded value. This offset is quantified and utilized as the basis for ranking.

By projecting the high-dimensional FPR onto a one-dimensional subspace, the FPR of parameter p_0 can be expressed as:

$$\Omega = [\omega_{\min}, \omega_{\max}] = \{p_0 \in \Re^{N_p} \,/\, \omega_{\min} \le p_0 \le \omega_{\max}\} \tag{23}$$

The length of the FPR of p_0 is given by $L(\Omega) = \omega_{\max} - \omega_{\min}$.

The minimum distance $d_{\min}$ between p_0 and the boundary of the corresponding FPR is quantified as:

$$d_{\min}(p_0, \Omega) = \begin{cases} \omega_{\min} - p_0 & p_0 < \omega_{\min} \\ \min(p_0 - \omega_{\min}, \omega_{\max} - p_0) & p_0 \in \Omega \\ p_0 - \omega_{\max} & p_0 > \omega_{\max} \end{cases} \tag{24}$$

The normalized distance ρ is given by:

$$\rho(p_0, \Omega) = \frac{d_{\min}(p_0, \Omega)}{L(\Omega)} \tag{25}$$

The criticality index γ is defined to quantify borderline cases:

$$\gamma(p_0, \Omega, \varepsilon) = \begin{cases} 1 & p_0 \notin \Omega \\ \max\left(0, 1 - \dfrac{\rho(p_0, \Omega)}{\varepsilon}\right) & p_0 \in \Omega \end{cases} \tag{26}$$

where ε is the critical threshold, with values ranging from 0.05 to 0.1 in this paper.

The parameters are then sorted according to the severity index S which is formulated as:

$$S(p_0, \Omega) = \begin{cases} 2 + \rho(p_0, \Omega) & p_0 \notin \Omega \\ 1 + \gamma(p_0, \Omega, \varepsilon) & p_0 \in \Omega \end{cases} \tag{27}$$

If $S_1(p_1, \Omega) > S_2(p_2, \Omega)$, the parameter associated with S_1 is prioritized for correction.

The parameters in *SP* are ranked according to the value of the S-index and categorized into three priority levels: level I (immediate correction), level II (high-priority inspection), and level III (monitor only), as shown in Fig. 2.

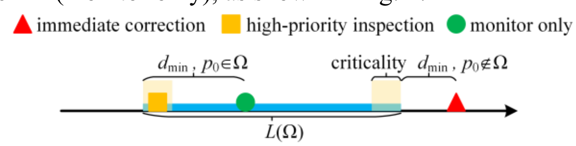

Figure 2. Position of the three priority-level parameters relative to the FPR.

C. Stage 3 Detailed Analysis

Stage 3 performs a detailed analysis, encompassing PE and correction validation. The top-ranked parameters are first estimated and subsequently corrected by augmenting the selected suspicious parameters to the state vector and solving the WLS estimation problem:

$$\min J(\boldsymbol{x}_{\mathrm{a}}) = [\boldsymbol{z} - \boldsymbol{h}(\boldsymbol{x}, \boldsymbol{p})]^{\mathrm{T}} \boldsymbol{R}^{-1} [\boldsymbol{z} - \boldsymbol{h}(\boldsymbol{x}, \boldsymbol{p})] \tag{28}$$

To ensure algorithmic convergence, PE is solved using the trajectory-unified (TJU)-based method [13], which comprises a dynamic phase and a static phase. The first part corresponds to the QGS solution phase, which traces the RSEM. The second part comprises the Gauss-Newton solution phase, which iteratively solves the PE problem. The QGS method exhibits global convergence, while the Gauss-Newton method provides rapid local convergence. In this work, PE is initialized from the feasible solutions derived from the FPR, which represents the RSEM obtained in the ranking stage.

Following this, multiple-snapshot SEs are performed again using the updated line parameters values. If residual satisfies the required criteria, the identification and correction results are validated, and the process terminates; otherwise, the parameters from the next priority level (e.g., level II) are incorporated into the current selected parameters. All parameters within this expanded selection are then estimated simultaneously, initialized from their recorded values. If residual violations remain after all parameters in *SP* have been analyzed, the method returns to

979-8-3315-8138-1

Stage 1. In this new iteration, α and φ_j are adaptively adjusted, leading to the regeneration of *SP*.

IV. Numerical Studies

In this section, the proposed method is evaluated on the IEEE 14-bus and 118-bus systems. For the analysis, 200 measurement snapshots are generated by adding normally distributed noise to power flow solutions derived from load conditions varying between 0.8 and 1.2 times their nominal values.

A. IEEE 14-Bus System

The standard error deviations are set to $\sigma_{\mathrm{PF}} = \sigma_{\mathrm{PI}} = 0.003$ p.u., $\sigma_{\mathrm{QF}} = \sigma_{\mathrm{QI}} = 0.005$ p.u., and $\sigma_{\mathrm{VM}} = 0.001$ p.u.

1) Case 1: Multiple Nonadjacent Parameter Errors

The erroneous parameter set $\{r_{1\text{-}2}, x_{3\text{-}4}, b_{6\text{-}11}\}$ is constructed by introducing multiple errors into parameters of nonadjacent lines: 1) a +20% error to $r_{1\text{-}2}$, 2) a +20% error to $x_{3\text{-}4}$, and 3) a +0.005 p.u. error to $b_{6\text{-}11}$.

The screening stage (Stage 1) identifies a suspicious parameter set (SP) containing 15 parameters. $SP = \{r_{1\text{-}2}, x_{1\text{-}2}, r_{1\text{-}5}, x_{1\text{-}5}, r_{2\text{-}3}, r_{2\text{-}4}, x_{2\text{-}4}, r_{2\text{-}5}, x_{2\text{-}5}, r_{3\text{-}4}, x_{3\text{-}4}, r_{4\text{-}5}, x_{4\text{-}5}, r_{5\text{-}6}, b_{6\text{-}11}\}$. The ranking stage (Stage 2) then characterizes the FPR for these parameters and applies the *S*-index, as shown in Fig. 3.

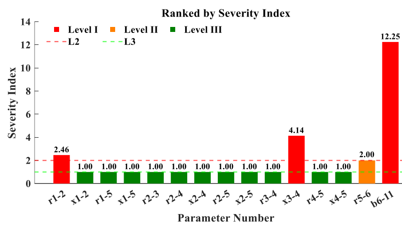

Figure 3. *S*-index of the suspicious parameters in the IEEE 14-bus system with multiple nonadjacent parameter errors.

The parameters ranked as level I are augmented into the state vector, and the combined parameter-state estimation problem is solved. The results in Table I demonstrate that all the three erroneous parameters are correctly identified as level I and effectively corrected in the detailed analysis stage (Stage 3).

TABLE I. Parameters with Multiple Nonadjacent Errors

Param.	Recorded(p.u.)	True(p.u.)	Estimated(p.u.)	Correction
$r_{1\text{-}2}$	0.02326	0.01938	0.01937	20.072%
$x_{3\text{-}4}$	0.20524	0.17103	0.17097	20.037%
$b_{6\text{-}11}$	0.00500	0.00000	0.00041	N/A

[1] **Correction**: The achieved correction magnitude relative to the true value, calculated as (|Recorded − Estimated| / True) × 100%.
[2] N/A: The metric is undefined due to division by zero.

2) Case 2: Multiple Adjacent Parameter Errors

A set of four test scenarios is designed to evaluate robustness, each characterized by a specific relative error (15%, 20%, 25%, or 30%) applied concurrently to parameters $r_{2\text{-}3}$, $r_{2\text{-}4}$ and $r_{2\text{-}5}$, which belong to adjacent lines. The screening stage establishes a corresponding suspicious parameter set *SP* for each parameter error level. After characterizing the FPRs of these parameters, the parameters in *SP* are ranked based on the *S*-index, as presented in Fig. 4.

The level I parameters are estimated first by solving the combined parameter-state estimation problem. As shown in Table II, the method correctly identifies and corrects all adjacent errors in a single iteration, with substantial correction magnitudes confirming the effectiveness of the proposed method. Furthermore, these results demonstrate the ability of the proposed method to accurately identify multiple adjacent line parameter errors, showing robustness against the similar error patterns of resistance r and reactance x.

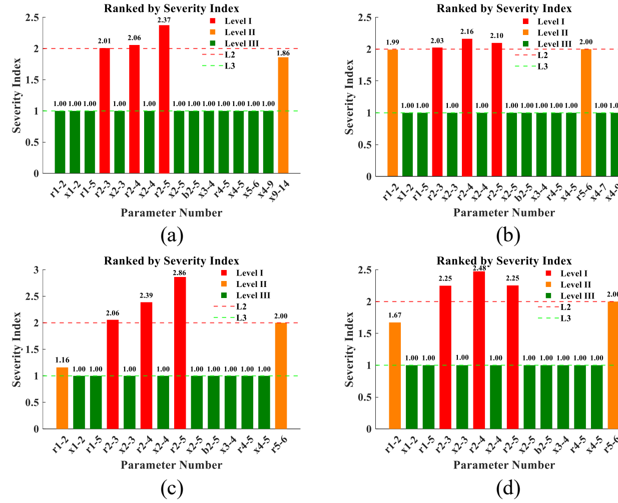

Figure 4. *S*-index of the suspicious parameters in the IEEE 14-bus system with multiple adjacent parameter errors under different error levels. (a)15%, (b)20%, (c)25%, (d)30% relative errors.

To evaluate the precision of the corrections, the estimation error relative to the true value is calculated. The high precision of the TJU-based method is demonstrated by estimation errors remaining at or below 0.086% in most cases, with the maximum observed estimation error being 0.123% for parameter $r_{2\text{-}5}$ under the 15% error scenario.

TABLE II. Parameter Correction Result with Multiple Adjacent Errors

Error	Param.	Recorded(p.u.)	True(p.u.)	Estimated(p.u.)	Correction
15%	$r_{2\text{-}3}$	0.05404	0.04699	0.04700	14.982%
	$r_{2\text{-}4}$	0.06683	0.05811	0.05815	14.937%
	$r_{2\text{-}5}$	0.06549	0.05695	0.05688	15.119%
20%	$r_{2\text{-}3}$	0.05639	0.04699	0.04700	19.983%
	$r_{2\text{-}4}$	0.06973	0.05811	0.05816	19.911%
	$r_{2\text{-}5}$	0.06834	0.05695	0.05691	20.070%
25%	$r_{2\text{-}3}$	0.05874	0.04699	0.04699	25.005%
	$r_{2\text{-}4}$	0.07264	0.05811	0.05814	24.953%
	$r_{2\text{-}5}$	0.07119	0.05695	0.05691	25.075%
30%	$r_{2\text{-}3}$	0.06109	0.04699	0.04699	30.006%
	$r_{2\text{-}4}$	0.07554	0.05811	0.05814	29.943%
	$r_{2\text{-}5}$	0.07404	0.05695	0.05691	30.079%

B. IEEE 118-Bus System

The standard error deviations are set to $\sigma_{\mathrm{PF}} = \sigma_{\mathrm{PI}} = \sigma_{\mathrm{QF}} = \sigma_{\mathrm{QI}} = \sigma_{\mathrm{VM}} = 0.005$ p.u. Multiple parameter errors are added to 10 adjacent lines and the erroneous parameter set $\{x_{39\text{-}40}, x_{40\text{-}41}, x_{40\text{-}42}, x_{41\text{-}42}, x_{43\text{-}44}, x_{24\text{-}70}, x_{70\text{-}71}, x_{24\text{-}72}, x_{71\text{-}72}, x_{71\text{-}73}\}$ is constructed.

25 parameters are declared after the screening stage, forming the suspicious parameter set *SP*. Based on the FPR corresponding to the parameters in *SP*, the *S*-index is calculated and used to prioritize these parameters. Fig.5 presents the resulting ranking.

Based on the augmented state vector incorporating the level I-ranked parameters, the parameter values are estimated by solving the combined parameter-state estimation problem, with the results presented in Table III. It is observed that all erroneous parameters are accurately identified without any missed detections and are effectively corrected.

979-8-3315-8138-1

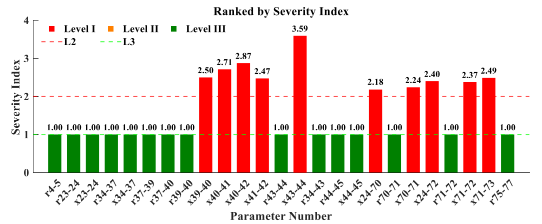

Figure 5. *S*-index of the suspicious parameters in the 118-bus systems.

TABLE III. IEEE 118-BUS SYSTEM WITH MULTIPLE PARAMETER ERRORS

Param.	Recorded (p.u.)	True (p.u.)	Proposed method		Method in [14]	REL.IMP.
			Estimated(p.u.)	Correction		
$x_{39\text{-}40}$	0.07050	0.06050	0.06031	16.843%	**0.06050**	N/A
$x_{40\text{-}41}$	0.05870	0.04870	0.04863	20.678%	**0.04868**	-2.512
$x_{40\text{-}42}$	0.21300	0.18300	**0.18412**	15.781%	0.18108	0.417
$x_{41\text{-}42}$	0.16500	0.13500	0.13918	19.126%	**0.13351**	-1.804
$x_{43\text{-}44}$	0.29540	0.24540	**0.24584**	20.196%	0.24458	0.464
$x_{24\text{-}70}$	0.49150	0.41150	**0.41225**	19.259%	0.40873	0.730
$x_{70\text{-}71}$	0.04550	0.03550	**0.03576**	27.437%	—	—
$x_{24\text{-}72}$	0.23600	0.19600	**0.19599**	20.413%	0.18523	0.999
$x_{71\text{-}72}$	0.22000	0.18000	**0.17943**	22.539%	0.16426	0.964
$x_{71\text{-}73}$	0.05540	0.04540	**0.04539**	22.048%	—	—

[1] **REL.IMP.**: Relative Improvement in estimation accuracy, calculated as (estimation error $_{[14]}$ – estimation error $_{\text{proposed}}$) / estimation error $_{[14]}$, where estimation error is (|True – Estimated| / True) × 100%.

The high capability in PEIC of the proposed method can be quantified by the relative improvement (REL.IMP.) metric over the method in [14]. Although the method in [14] demonstrates superior accuracy on three parameters, specifically achieving marginally lower errors for $x_{40\text{-}41}$ and $x_{41\text{-}42}$ while attaining perfect estimation for $x_{39\text{-}40}$, the proposed method maintains highly competitive performance in these cases, as evidenced by its estimation error of only 0.144% for $x_{40\text{-}41}$. For all other parameters, the proposed method consistently achieves superior accuracy, demonstrating the high precision of the proposed method.

C. Comparative Analysis of State Estimation Following PEIC

Comparative tests are conducted on two systems: the 14-bus system using the 30% error scenario within case 2, and the 118-bus system under the configurations described in Section IV.*B*.

TABLE IV. MULTIPLE-SNAPSHOT SES PERFORMANCE COMPARISONS

Test system	Evaluation metric	Method				Without parameter error
		Without PEIC	NLM method [9]	Method in [14]	Proposed method	
14-bus system	$J(x)$	385.60895	205.53709	89.24138	**88.44032**	88.78329
	$RMSE$(p.u.)	0.00441	0.00330	**0.00291**	0.00292	0.00291
	$MaxAE$(p.u.)	0.00804	0.00663	0.00569	**0.00566**	0.00567
118-bus system	$J(x)$	1362.57820	1141.38847	879.82996	**859.24493**	857.82083
	$RMSE$(p.u.)	0.00178	0.00175	0.00165	**0.00160**	0.00159
	$MaxAE$(p.u.)	0.00751	0.00739	0.00734	**0.00721**	0.00721

[1] **RMSE** (p.u.): The root mean square error.
[2] **MaxAE** (p.u.): The maximum absolute error of voltage magnitudes.

The multiple-snapshots WLS SE results summarized in Table IV demonstrate that the involved PEIC methods offer substantial improvement over the uncorrected case, as evidenced by reduced $J(x)$ and enhanced voltage estimation accuracy. Furthermore, the proposed method leads to the SE performance closest to that achieved with perfectly accurate parameters, a result enabled by its delivery of the most precise PEIC.

In addressing multiple adjacent parameter errors, the proposed method ensures correct identification, whereas the sequential estimation framework of the NLM method introduces identification errors. For the 14-bus system, several correct parameters $r_{1\text{-}2}$, $x_{1\text{-}2}$, $x_{1\text{-}5}$, $x_{2\text{-}3}$, $x_{2\text{-}4}$, $x_{2\text{-}5}$, $x_{4\text{-}5}$ are misidentified and erroneously estimated. For the 118-bus system, 10 correct parameters (e.g., $x_{37\text{-}39}$, $r_{37\text{-}40}$, $x_{34\text{-}43}$, $r_{44\text{-}45}$) are incorrectly identified and estimated with wrong values, while the actual erroneous parameters $x_{40\text{-}41}$, $x_{40\text{-}42}$, $x_{71\text{-}73}$ remained undetected. Errors in PEIC degrade the model accuracy, compromising the reliability of EMS advanced applications (e.g., optimal power flow).

V. CONCLUSION

This paper proposes a Feasible parameter region (FPR)-based parameter error identification and correction method to improve the accuracy of transmission line parameters. Numerically speaking, the proposed method was able to accurately identify the parameter errors (>10%) in all of the numerical studies. The FPR is completely characterized by employing the globally convergent QGS-based method. Building on this FPR characterization, erroneous transmission line parameters are accurately identified with a distinguishing property of mitigating the mutual interference among multiple adjacent parameter errors. A novel three-stage framework for PEIC has been proposed and validated via improved accuracy in state estimation. The parameters ranked as level I in the proposed three-stage method are augmented into the state vector to be estimated, and the combined parameter-state estimation problem is then solved to obtain the correct parameter values.

REFERENCES

[1] A. Monticelli. *State Estimation in Electric Power Systems*: *A Generalized Approach*. Massachusetts: Kluwer Academie Publishers, 1999.

[2] A. Abur and A. Gómez Expósito, *Power System State Estimation*: *Theory and Implementation*. New York, NY, USA: Marcel Dekker, 2004.

[3] V. H. Quintana and T. Van Cutsem, "Power system network parameter estimation," *Opt*. *Control Appl*. *Methods*, vol. 9, no. 3, pp. 303–323, 1988.

[4] W. Liu, F. Wu, and S. Lun, "Estimation of parameter errors from measurement residuals in state estimation," *IEEE Trans*. *Power Syst*., vol. 7, no. 1, pp. 81–89, Feb. 1992.

[5] W. -H. E. Liu and S. -L. Lim, "Parameter error identification and estimation in power system state estimation," *IEEE Trans*. *Power Syst*., vol. 10, no. 1, pp. 200-209, Feb. 1995.

[6] I. W. Slutsker, S. Mokhtari, and K. A. Clements, "Real time recursive parameter estimation in energy management system," *IEEE Trans*. *Power Syst*., vol. 11, no. 3, pp. 1393–1399, Aug. 1996.

[7] O. Alsac, N. Vempati, B. Stott, and A. Monticelli, "Generalized state estimation," *IEEE Trans*. *Power Syst*., vol. 13, no. 3, pp. 1069–1075, Aug. 1998.

[8] P. Zarco and A. G. Exposito, "Power system parameter estimation: A survey," *IEEE Trans*. *Power Syst*., vol. 15, no. 1, pp. 216–222, Feb. 2000.

[9] J. Zhu and A. Abur, "Identification of network parameter errors," *IEEE Trans*. *Power Syst*., vol. 21, no. 2, pp. 586–592, May 2006.

[10] Y. Lin and A. Abur, "A New framework for detection and identification of network parameter errors," *IEEE Trans*. *Smart Grid*, vol. 9, no. 3, pp. 1698-1706, May 2018.

[11] Y. Lin and A. Abur, "Strategic use of synchronized phasor measurements to improve network parameter error detection," *IEEE Trans. Smart Grid*, vol. 9, no. 5, pp. 5281-5290, Sept. 2018.

[12] H. D. Chiang and C. Y. Jiang, "Feasible region of optimal power flow: Characterization and applications," *IEEE Trans*. *Power Syst*., vol. 33, no. 1, pp. 236–244, Jan. 2018.

[13] J. J. Deng, H. D. Chiang, and T. Q. Zhao, "Newton method and trajectory-based method for solving power flow problems: Nonlinear studies," *Int*. *J*. *Bifurcat*. *Chaos*, vol. 25, no. 06, 2015, Art. no. 1530018.

[14] D. Liang, L. Zeng and H. D. Chiang, "Simultaneous identification and correction of multiple network parameter errors by mixed-effects models," *IEEE Trans*. *Control*. *Netw*. *Syst*., vol. 9, no. 2, pp. 879–890, June 2022.